Communications

Ultrawideband Printed-Circuit Antenna

K. Rambabu, H. A. Thiart, J. Bornemann, *Fellow, IEEE*, and S. Y. Yu

***Abstract*—The design of a novel ultrawideband printed-circuit antenna is presented. By using a stepped-patch in combination with multiple resonating elements, a bandwidth of more than 150% is obtained. The performance is demonstrated through measurements and calculations with a commercially available field solver. A phase center analysis shows very small variations over the entire available bandwidth.**

***Index Terms*—Multiresonance antennas, phase center, printed-circuit antennas, ultrawideband antennas (UWB).**

I. Introduction

Although tentative definitions of ultrawideband (UWB) applications refer to a minimum bandwidth of only 25% [1], antennas with much broader performances have been proposed recently. Broadband behavior can be achieved by well-known techniques such as the zigzag approach, e.g., [2]. However, in order to be more in tune with handheld devices for wireless applications, printed-circuit approaches are predominantly investigated. Planar antennas with L-shaped probes [3] or E-shaped patches [4] achieve bandwidths better than 30%. Overlapping patches use different resonances to obtain bandwidths beyond 50% [5]. Microstrip slot antennas [6] and triangular monopole antennas [7] can be designed for more than 80% bandwidth. Of particular interest is a combination of the stepped and slotted patch [8]. It leads to a simple and miniaturized design providing a VSWR and gain (>0 dB) bandwidth of 120% and 100%, respectively.

This paper focuses on a design for future UWB handsets, which combines the stepped-patch approach with a number of resonating elements, and achieves a bandwidth ($\mathrm{VSWR} < 2, \mathrm{gain} > 1$ dBi) of more than 150%.

II. UWB Antenna Design

The principal layout of the UWB antenna proposed in this paper is shown in Fig. 1. It is fed by a standard 50 Ω microstrip line and opens to a stepped patch at the point where the ground plane is removed. This is very similar to the circuit presented in [8]. However, instead of using a single slot in the patch, we are improving the gain and bandwidth of the antenna by systematically adding resonators of different lengths along the line. These resonators are arranged both vertically and horizontally and are fed through direct electrical connection.

The individual resonators are printed half-wave dipoles and are designed as follows. First, the resonator frequencies are chosen such that the bandwidth of resonator i will extend into that of resonator $i+1$. In this design, nine resonators are employed to cover the fundamental band from 6 to 22 GHz, and their harmonics will cover the band up to 45 GHz. The fundamental resonant frequencies are uniformly spaced, i.e., 6 to 22 GHz in steps of 2 GHz. As an example, let the resonant frequency of a resonator be 14 GHz. Assuming a substrate with $\varepsilon_r = 4.4$ (e.g., FR4), the half-wavelength of a printed dipole without ground plane is 5.8 mm, which is reduced to 5.1 mm as an effect of fringing fields (compare to r_1 below).

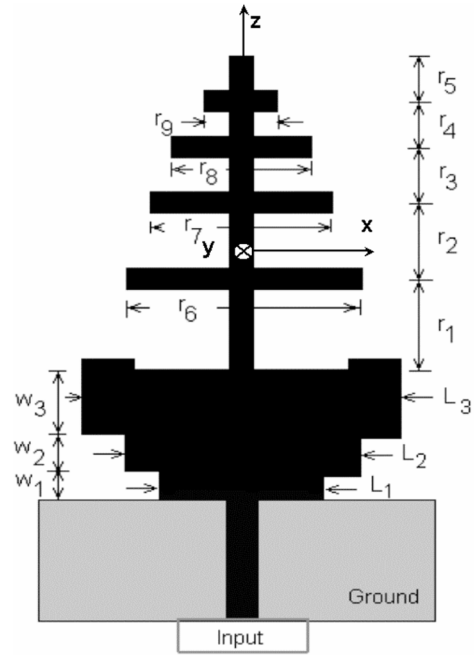

Fig. 1. UWB printed-circuit antenna.

In order to improve the bandwidth, a large number of resonators could be added in principle. For technical applications, however, a compromise between antenna size and UWB performance must be reached.

The current design (Fig. 1) was performed for FR4 substrate with $\varepsilon_\mathrm{r} = 4.4$ and height $\mathrm{h} = 1.58$ mm. The dimensions of the ground plane are 30 mm × 11.5 mm, those of the feed structure are $\mathrm{L}_1 = 9$ mm, $\mathrm{w}_1 = 1$ mm, $\mathrm{L}_2 = 12$ mm, $\mathrm{w}_2 = 1.5$ mm, $\mathrm{L}_3 = 15$ mm, and $\mathrm{w}_3 = 3.5$ mm. The width of the 50 Ω microstrip line is 3 mm. The lengths of the various resonators are $\mathrm{r}_1 = 5.1$ mm, $\mathrm{r}_2 = 4.8$ mm, $\mathrm{r}_3 = 4.5$ mm, $\mathrm{r}_4 = 4.2$ mm, $\mathrm{r}_5 = 4$ mm, $\mathrm{r}_6 = 12$ mm, $\mathrm{r}_7 = 9$ mm, $\mathrm{r}_8 = 7.1$ mm and $\mathrm{r}_9 = 6$ mm. The widths of all resonators are 1 mm. The two small pedestals between dimensions w_3 and r_1 are used for matching purposes. Their dimensions are 2 mm in x and 0.5 mm in z direction. Note that scaled versions of this antenna provide excellent initial designs for operation in other frequency ranges.

The actual length of the antenna, excluding the ground plane, is 30 mm as shown in the photograph (Fig. 2). A substrate with dimensions of 48 mm × 31 mm has been used for the prototype. Note that the size is small enough for integration in modern wireless handheld devices. However, since ground planes nearby largely affect the antenna's behavior, it is recommended that it be placed on top of the device.

Manuscript received April 10, 2005; revised May 17, 2006.

K. Rambabu was with the Department of Electrical and Computer Engineering, University of Victoria, Victoria, BC V8W 3P6, Canada. He is now with the Institute for Infocomm Research, Singapore Science Park II, Singapore 117674, Singapore.

H. A. Thiart was with the Department of Electrical and Computer Engineering, University of Victoria, Victoria, BC V8W 3P6, Canada. He is now with Adventenna Inc., Santa Clara, CA 95054 USA.

J. Bornemann and S. Y. Yu are with the Department of Electrical and Computer Engineering, University of Victoria, Victoria, BC V8W 3P6, Canada.

Digital Object Identifier 10.1109/TAP.2006.886568

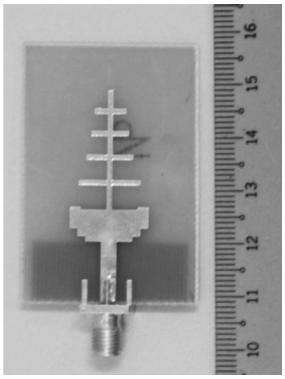

Fig. 2. Photograph of the UWB antenna prototype and size comparison with a metric ruler.

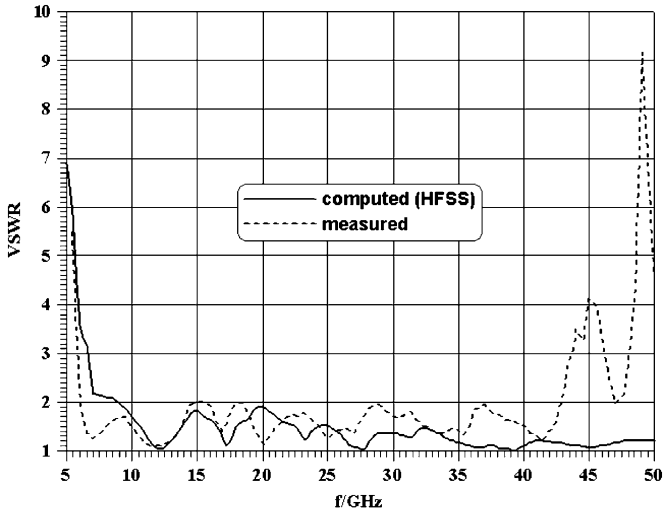

Fig. 3. Measured and simulated VSWR of UWB antenna.

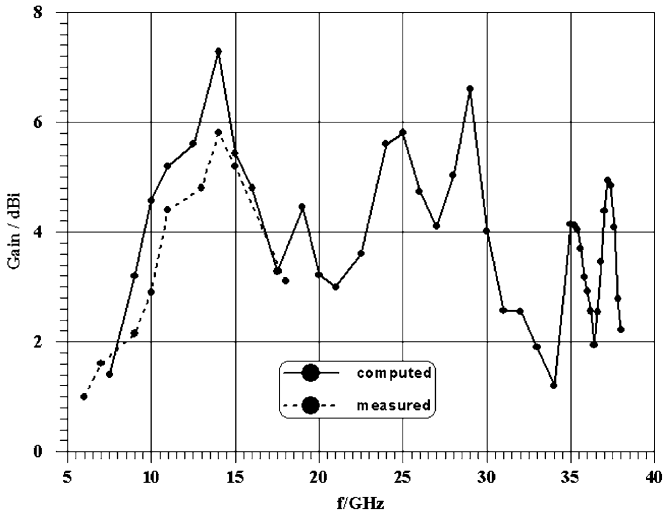

Fig. 4. Computed and measured gain of UWB antenna.

Computer simulations near the individual resonant frequencies (not shown here) reveal that the currents in the vertical resonators slightly extend into the adjacent horizontal ones, and vice versa. Therefore, the radiation is occurring from two perpendicular conductors over significant stretches of the frequency range which gives rise to a dual-polarization performance. This is considered an asset in mobile wireless communications, due to the frequent movement of handsets and reflections from buildings and other obstacles.

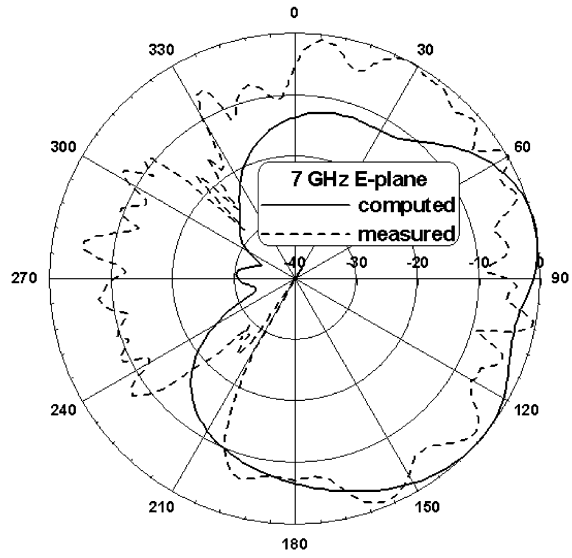

Fig. 5. Computed and measured normalized (a) E-plane and (b) H-plane radiation patterns of UWB printed-circuit antenna at 7 GHz.

III. Results

The UWB antenna specified above has been analyzed by the commercially available field solver HFSS. A prototype (Fig. 2) was fabricated and measured using facilities specified up to 18 GHz.

Fig. 3 shows the comparison between computed and measured VSWR of the prototype. The measured frequencies for $\mathrm{VSWR} < 2$ are 6 GHz and 42.8 GHz, thus resulting in a bandwidth of 150.8%. Although the simulation predicts an even larger bandwidth (up to 50 GHz), the measurement deviates from the calculation above 43 GHz. This is mainly due to the 40 GHz connector used and the fact that the permittivity of the FR4 substrate material varies significantly in the millimeter-wave frequency range.

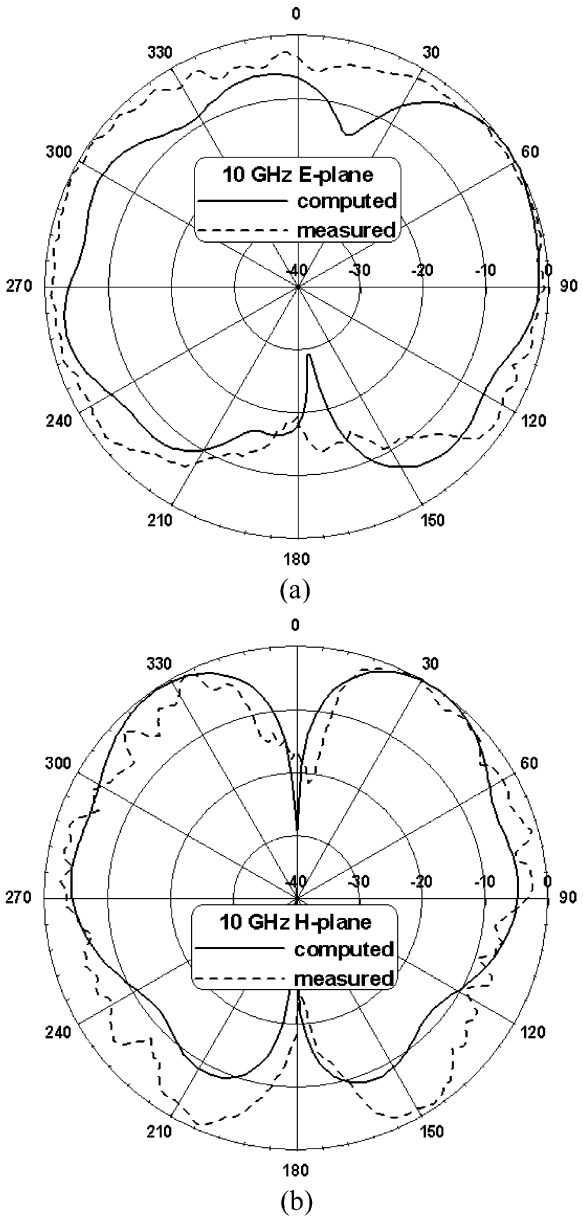

Fig. 6. Computed and measured normalized (a) E-plane and (b) H-plane radiation patterns of UWB printed-circuit antenna at 10 GHz.

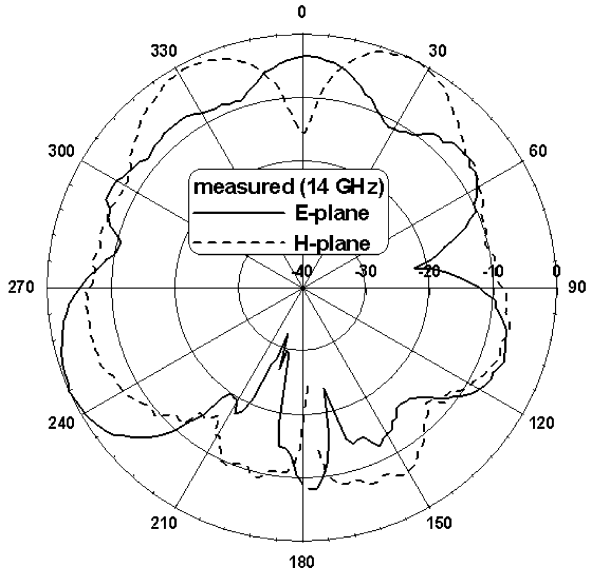

Fig. 7. Measured normalized E-plane (solid line) and H-plane (dashed line) radiation patterns of UWB printed-circuit antenna at 14 GHz.

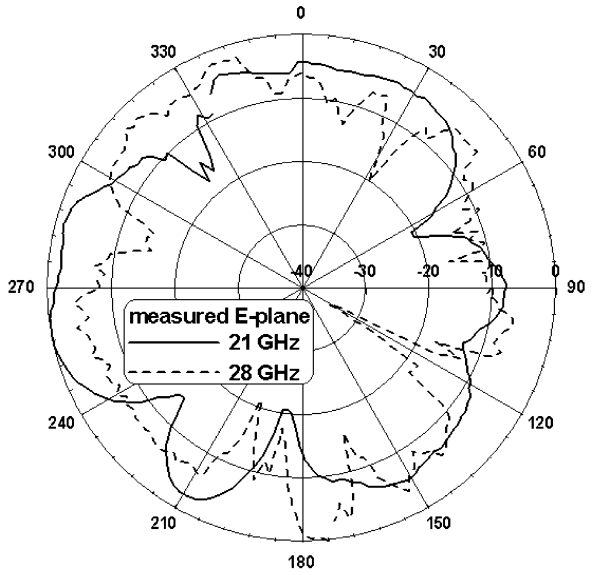

Fig. 8. Measured normalized E-plane radiation patterns of UWB antenna at 21 GHz (solid line) and 28 GHz (dashed line).

Due to memory limitations of 2 GB, gain computations had to be aborted at 38 GHz. The gain performance is shown in Fig. 4 and demonstrates a variation similar to other wideband antennas. However, the gain does not drop below 1 dBi and, therefore, this design is an improvement over that presented in [8]. The measured gain is shown in Fig. 4 at nine different frequencies up to 18 GHz. Although it is slightly lower than computed, it confirms the general frequency dependence of the computations.

Fig. 5 through 9 show the normalized radiation patterns at selected frequencies. Assuming the conventional definition of angles θ and ϕ, we define the E-plane as the yz-plane (Fig. 1) and plot $\mathrm{E}_\theta(\phi = \pi/2)$. This is commonly referred to as the co-polarized E-plane. In order to demonstrate the dual-polarization character of this antenna, the H-plane (xz-plane) plots show $\mathrm{E}_\theta(\phi = 0)$, which corresponds to the cross-polar H-plane in conventional (narrowband and polarization-sensitive) applications. Note that this presentation is different from that in other published works on UWB antennas, e.g., [7], but it serves the purpose of demonstrating the dual-polarized character of radiation.

The main purpose of the radiation patterns is to demonstrate that the antenna actually radiates over a wide frequency band. The radiation patterns vary considerably with frequency, which is commonly accepted in UWB applications [7]. Reasonable agreement between computations and measurements is demonstrated at 7 GHz (Fig. 5) and 10 GHz (Fig. 6). Similar agreement is obtained at higher frequencies. Therefore, Fig. 7 only shows measured E- and H-plane patterns at 14 GHz, and Fig. 8 shows measured E-plane patterns at 21 GHz and 28 GHz. Note that the antenna is symmetric in the H-plane, thus producing nearly symmetric measured patterns. It is asymmetric in the E-plane due to the fact that ground plane and radiating elements are located on opposite sides of the substrate. Therefore, only measured E-plane patterns are shown at 21, 28 GHz (Fig. 8).

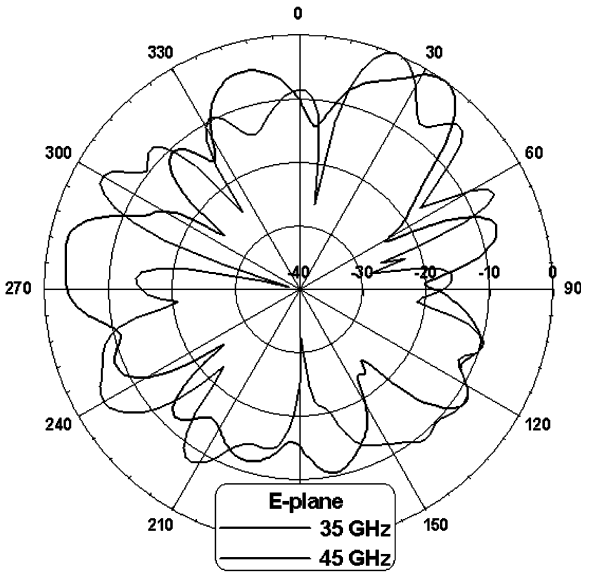

Fig. 9. Computed normalized E-plane radiation patterns of UWB printed-circuit antenna at 35 and 45 GHz.

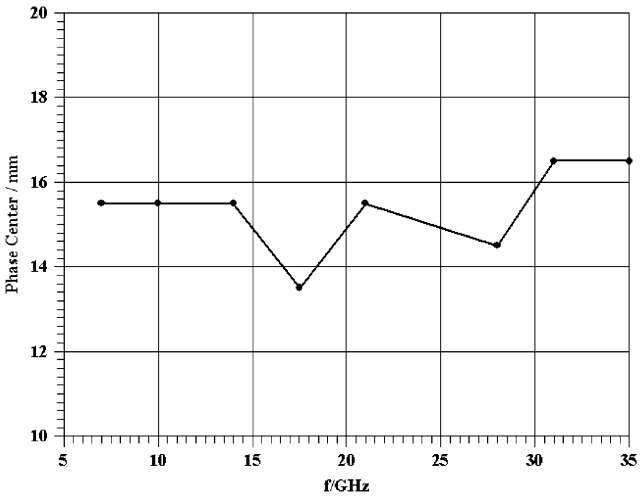

Fig. 10. Computed phase center location versus frequency. The reference point is at the input shown in Fig. 1.

Since frequencies in Fig. 8 are beyond the specifications of the facility (top of Section III), measurement accuracy had to be severely sacrificed in order to obtain the data. Therefore, and because of grounding problems in the measurement setup, the measured values in Fig. 8 and the computed E-plane patterns at 35, 45 GHz in Fig. 9 merely serve the purpose to demonstrate that radiation takes place.

Pattern minima occur over the entire frequency range, but only in certain directions and not over an entire sector. Since the application of this antenna is primarily for handheld devices, where movement and reflections occur naturally, the minima are not considered to be detrimental to overall performance.

Since UWB antennas involve radiation of pulses, the variation of the phase center is an important performance criterion. Ideally, all frequencies contained in the pulse are radiated from the same point (phase center).

Therefore, all frequencies travel the same distance in the same time, and the pulse can be received undistorted. In practice, however, the phase center varies with frequency along the antenna surface (or axis) and gives rise to the term "apparent phase center" for most regular medium bandwidth antennas. In order to quantify this behavior, either the group delay (e.g., [8]) or the frequency-dependent phase-center location can be plotted. To determine the phase-center variation of this UWB design, a reference point on the antenna is chosen, and the phase variation in the near field over the main beam is computed for different phase center points moved from the reference point along the axis of the antenna. A valid phase center location is chosen if the phase variation over the main beam is within three degrees. Fig. 10 shows that the phase center variation is within three millimeters over the entire frequency band. Since the reference point is set at the input of the antenna (i.e., where the ground plane is removed in Fig. 1), the phase center is located within the section denoted by r_2 in Fig. 1.

IV. Conclusion

The antenna design presented in this paper presents a viable option for future UWB handset applications. With a bandwidth of 150%, a gain of better than 1 dBi and only a small phase center variation, this design is capable of handling pulsed propagation with frequency components up and into the millimeter-wave regime. Measurements confirm the design procedure and basic operation of the antenna.

Acknowledgment

The pattern and gain measurements were performed at the Institute for Infocomm Research $(\mathrm{I}^2\mathrm{R})$ in Singapore. The authors are greatly indebted to the members of $\mathrm{I}^2\mathrm{R}$ for letting them use their facility.

References

[1] B. Pattan, "A brief exposure to ultra-wideband signaling," *Microwave J.*, vol. 46, pp. 104–110, Dec. 2003.

[2] S. K. Sharma and L. Shafai, "Investigations on miniaturized endfire vertically polarized quasi-fractal log-periodic zigzag antenna," *IEEE Trans. Antennas Propag.*, vol. 52, pp. 1957–1962, Aug. 2004.

[3] C. L. Mak, K. M. Luk, K. F. Lee, and Y. L. Chow, "Experimental study of microstrip patch antenna with an L-shaped probe," *IEEE Trans. Antennas Propag.*, vol. 48, pp. 777–783, May 2000.

[4] F. Yang, X.-X. Zhang, X. Ye, and Y. Rahmat-Samii, "Wide-band E-shaped patch antennas for wireless communications," *IEEE Trans. Antennas Propag.*, vol. 49, pp. 1094–1100, Jul. 2001.

[5] K. Rambabu, M. Alam, J. Bornemann, and M. A. Stuchly, "Compact wideband dual-polarized microstrip patch antenna," in *IEEE AP-S Int. Symp. Dig.*, Monterey, CA, Jun. 2004, no. 75.7, p. 4.

[6] S. I. Latif and L. Shafai, "Wideband and reduced size microstrip slot antennas for wireless applications," in *IEEE AP-S Int. Symp. Dig.*, Monterey, CA, Jun. 2004, pp. 1959–1962.

[7] H. R. Chuang, C. C. Lin, and Y. C. Kan, "A printed UWB triangular monopole antenna," *Microwave J.*, vol. 49, pp. 108–120, Jan. 2006.

[8] S. H. Choi, J. K. Park, S. K. Kim, and J. Y. Park, "A new ultra-wideband antenna for UWB applications," *Microwave Opt. Technol. Lett.*, vol. 40, pp. 399–401, Mar. 2004.